Dual-mode Dual-band Microstrip Bandpass Filter with High Selection Performance

Hong-Shu Lu[1], **Qian Li**[2], **Jing-Jian Huang**[1], **Xiao-Fa Zhang**[1], **and Nai-Chang Yuan**[1]

[1]College of Electronic Science and Engineering, National University of Defense Technology
109 Deya Road, Changsha, Hunan 410073, China
[2]College of Remote Sensing and Information Engineering, Wuhan University
129 Luoyu Road, Wuhan, Hubei 430079, China

Abstract— In this letter, a new dual-mode microstrip bandpass filter (BPF) which is mainly composed of a dual-mode resonator, i.e., meandered loop resonator, with high selection performance is proposed. Compared with the traditional square loop resonator (SLR), meander loop resonator has more advantages in miniaturization. Besides, a Minkowski-like pre-fractal geometry with 1st order iteration embedded at the center of the resonator is utilized to improve the BPF capability. Both input and output ports are spatially separated 90° from each other. A small patch located in the orthogonal corner of the proposed resonator where is 135° offset from input and output ports is introduced to excite two degenerate modes. By tuning the perturbation, the two degenerate modes are excited. The influence of the variation of the perturbation size on the resonant frequencies and the coupling coefficient of the two degenerate modes is investigated. By observing the distribution of the surface current, it can be more intuitive to understand which part of the resonator has played a role when operating in different frequency bands.

1. INTRODUCTION

Microstrip bandpass filters (BPFs) are mainly used to filter out the signals within the specific frequency bands and suppress out of band spurious signals. As an indispensable component in the RF front end of multifarious modern electronic communication systems, microstrip bandpass filters (BPFs) play an important role in simplifying systems complexity and improving systems stability. Furthermore, microstrip BPFs have many attractive features, such as low loss, low lost, easy fabrication, small size, and so on. Duo to the rapid development of the wireless communication technology, the systems and modules gradually tend towards the direction of miniaturization and multifunction. Consequently, the market demand for microstrip BPFs with excellent performance and compact configuration is more and more strong.

Dual-mode BPF was firstly proposed using a dual-mode ring resonator by Wolff [1]. He explained that two degenerate modes could be excited by disturbing the symmetry of the resonator. What's more, utilizing the two degenerate modes could realize a double-tuned microstrip BPF. In other words, the dual-mode microstrip BPF can be used as a double circuit in single structure as compared to the signal mode microstrip BPF when the two degenerate modes are excited by some means. Therefore, the number of resonators required for a given degree of filter is reduced by half, resulting in a compact filter configuration. It is because the dual-mode resonators have the characteristics of miniaturization design, many researches on designing dual-mode BPFs have been carried out by a lot of academicians.

A ring resonator BPF with switchable passband bandwidth was presented in [2]. Interdigital-coupled feed lines were used in this proposed BPF to suppress harmonics by adding transmission zeros outside of the passband, resulting in wide upper and lower stopbands. M. Keshvari and M. Tayarani [3] applied the slow-wave transmission line concept which had been used effectively to reduce the physical size of the microwave components to design a compact dual-mode filter. The noticeable difference between a conventional square ring resonator and the proposed one is periodic shunt loading of square's sides with capacitive stubs to reduce the physical length of resonator. A miniaturized dual-mode BPF with a high selective performance for dual-band applications is presented in [4]. The filter is designed with square loop resonator with tree-shaped patches attached to the four inner corners of the loop, which equivalents to load capacitors in the inner of loop resonator. In order to design a dual-mode dual-band microstrip BPF with controllable center frequency, the dual-mode meandered loop resonator that having internally located square loop loading elements was harnessed by Ceyhun Karpuz et al. [5]. The center frequency of the designed BPF could shift up or down as the connection points of the loading elements changed.

Fractal curve, as an effective method to reject insertion loss and heighten selectivity, has been widely applied in the design of BPFs in recent years. The term fractal, which means broken or irregular fragments, was first defined by Mandelbrot [6] as a method of assorting structures whose dimensions were not complete numbers. Different from Euclidean geometries, fractal geometries have two common properties: space-filling and self-similarity, which are the reasons why the fractal design can be an attractive method to design and fabricate antennas and passive RF/microwave circuits. It has been shown that the self-similarity property of fractal shapes has been successfully applied to the design of multiband antennas in [7], while adopting the space-filling property of fractals can reduce the antenna size effectively.

A 3rd order Sierpinski fractal-based resonator (SFR) is applied to design a new microstrip dual-mode BPF centered at 2.4 GHz [8]. The different order SFRs are generated from the conventional square patch by using an iterative Sierpinski generator method. By increasing the iteration order of SFR, the resonator frequency can be moved towards the lower frequency, indicating a miniaturized property. Changing the edges of the foursquare complementary split-ring resonator (CSRR) into Koch fractal curve shape forms a new structure and a BPF has been designed based on the new structure [9]. The simulated results show that the fractal geometry can significantly lower the size of the structure. Moreover, the improved frequency selectivity in the upper transition band is achieved. A novel Moore curve fractal-shaped complementary spiral resonator (CSR) is proposed and analyzed in [10]. The metamaterial unit cell is realizing by using a microstrip line loaded with series gap discontinuities and implementing fractal shape CSR in ground plane that as a composite right left hand transmission line. Compared with Euclidean-shaped SRR and other fractal-shaped CSR namely the Hilbert curve CSR, 49% and 10% reduction in size miniaturization are obtained, respectively.

In this paper, a compact dual-mode dual-band microstrip BPF designed using dual-mode meander loop resonator with a high selective performance is presented. In order to improve the BPF capability, a MIB fractal structure with 1st order iteration is embedded at the center of the resonator, which means changing the values of the parasitic capacitance and inductance. By adjusting the dimension parameters of the resonator, center frequency, fractional bandwidth (FBW) and the frequency response of the designed BPF can be controlled. Moreover, degenerate modes can be excited by changing the perturbation size. The mode-splitting characteristic and impact of the perturbation on the performance of the BPF is investigated in details.

2. MEANDER LOOP RESONATOR

Figure 1 shows the typical schematic layouts of the symmetric dual-mode resonators which has been mentioned in [1, 3, 4], respectively. Compared with conventional ring resonator and square ring resonator, the meander loop resonator has advantage of compact size.

The guided wavelength λ_g at design frequency f_0 can be calculated from the equation [12]:

$$\lambda_g = \frac{c}{f_0 \cdot \sqrt{\varepsilon_{eff}}} \tag{1}$$

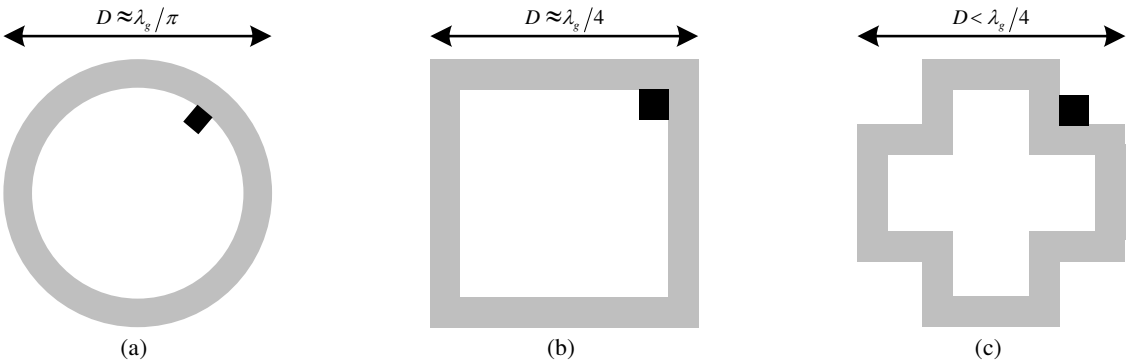

Figure 1: Typical dual-mode microstrip loop resonators. (a) Ring resonator; (b) Square ring resonator; (c) Meander loop resonator. (Gray areas indicate the metallic and black areas indicate the perturbation).

where c is speed of light and ε_{eff} is the effective dielectric constant, given by [12], as:

$$\varepsilon_{eff} = \frac{\varepsilon_r + 1}{2} \tag{2}$$

where ε_r is the dielectric constant of the substrate.

The typical dual-mode BPF based on meander loop resonator is shown in Fig. 2(a) by adding two T-shaped coupling feed lines. The corresponding elliptical filtering characteristic with two transmission zeros (TZs) is illustrated in Fig. 2(b). The two TZs are created because there is a parasitic coupling between the input and output. In addition to the two TZs, the mode splitting is clearly observed from the figure. This situation can also be seen from the coupling coefficient computed using the relationship between the split in the resonance frequency of two modes and the coupling, as described by [12]:

$$k = \frac{f_{02}^2 - f_{01}^2}{f_{02}^2 + f_{01}^2} \tag{3}$$

where f_{01} and f_{02} are the resonance frequency of mode I and mode II, respectively.

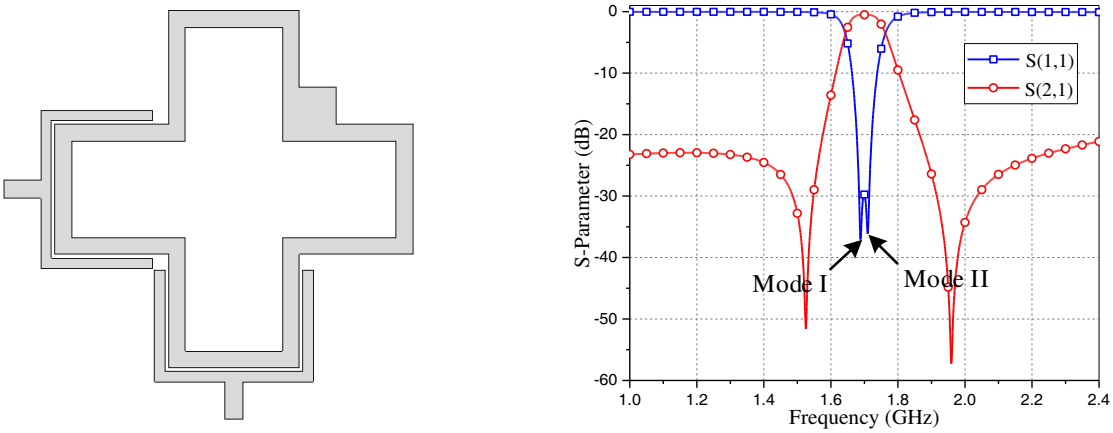

Figure 2: Typical dual-mode BPF with meander loop resonator and its elliptic response. (a) Configuration of typical dual-mode BPF with meander loop resonator; (b) The corresponding return loss and transmission responses.

3. FILTER DESIGN

In order to design a dual-mode dual-band BPF operating at 2.4 GHz and 3.5 GHz, applying a 1st iteration Minkowski-like pre-fractal structure, mentioned in [13], which will be embedded in the typical dual-mode BPF based on meander loop resonator to achieve this goal. The layout of the proposed BPF is depicted in Fig. 3(a). It is assumed that, the filter is designed on a RT/Duriod microwave board that has relative dielectric constant $\varepsilon_r = 10.8$, dielectric thickness $h = 1.27$ mm and thickness of copper layer $t = 35$ µm.

After the optical design process, the dimension parameters of the proposed BPF are chosen as follows:$L_1 = L_2 = 7$ mm, $L_3 = 0.85$ mm, $L_4 = 2$ mm, $W_1 = 0.9$ mm, $W_2 = 0.55$ mm, $W_3 = 0.98$ mm, $W_{p1} = W_{p2} = 2.6$ mm, $g = 0.2$ mm, and $a = 0.8$.

4. PERFORMANCE EVALUATION

The proposed BPF depicted in Fig. 3(a) has been modeled and analyzed by using CST Microwave Studio 2014. It is assumed that the conductor material is perfect conductor. Fig. 3(b) shows the corresponding return loss and transmission responses. It is clearly observed that two passbands with central frequencies locate at 2.407 GHz and 3.491 GHz, separately. At the lower passband, the simulated maximum insertion loss is 0.56 dB, the fractional bandwidth (FBW) is 7.3% and the return loss is better than −35 dB from 2.39 GHz to 2.42 GHz. The two TZs locate on both sides of the lower passband which are −51 dB and −58 dB at the frequencies of 2.145 GHz and 2.801 GHz respectively. Due to the present of the two TZs, the selectivity of the BPF as well as the stopband

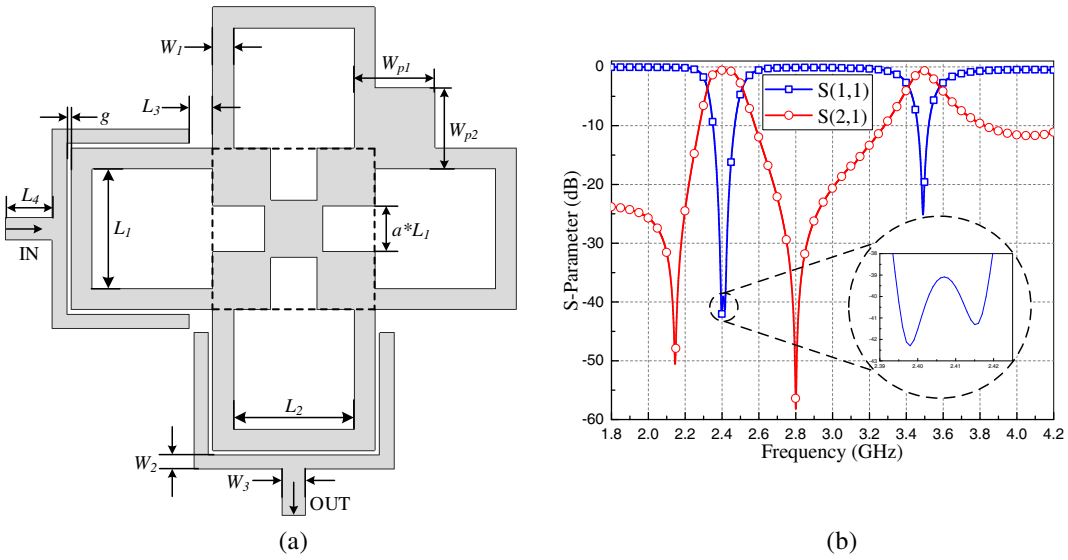

Figure 3: Layout of the dual-mode dual-band BPF and corresponding frequency characteristics. (a) Proposed configuration; (b) Simulated return loss and transmission responses (Gray areas indicate the metallic).

rejection can be improved effectively. Therefore, the proposed BPF can reduced the interferences from other systems. The maximum insertion loss is 0.62 dB and the FBW is 4.4% at the upper passband. Note that two degenerate modes are located at 2.398 GHz and 2.415 GHz separately within the lower passband.

Figure 4 shows the resonant frequencies of the degenerate modes and corresponding coupling coefficient versus the perturbation size which is changing from 2.55 mm to 3.15 mm. It is apparent that the degenerate modes appear when the perturbation size is larger than 2.55 mm and with the increasing of the perturbation size, the distance between the two modes resonant frequencies split becomes larger and accordingly the bandwidth expands. Furthermore, the coupling coefficient (k) increases too.

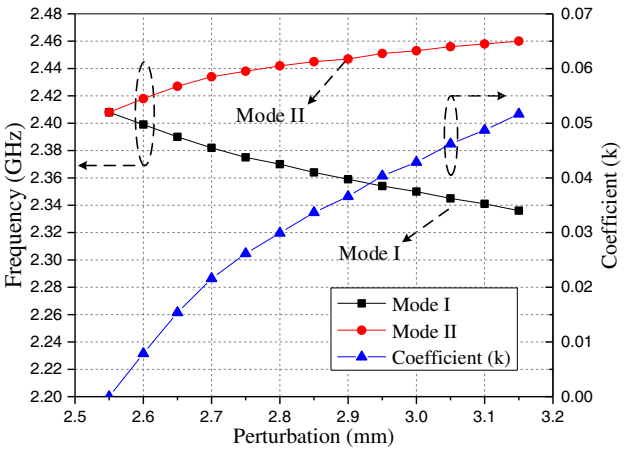

Figure 4: Resonant frequencies of the degenerate modes and coupling coefficient versus the perturbation size.

The surface current distributions of the proposed BPF are presented in Fig. 5. In these graphs, red color indicates the strong coupling effects while blue color indicates the weak ones. It is clear from Figs. 5(a) and (d) that the input signal is mostly reflected back at the input port and litter energy distributes at the output port at the two TZs located at 2.145 GHz and 2.801 GHz. While in Figs. 5(b), (c) and (e), the current flows through the input port is almost completely coupled to the output port in the two passbands located at 2.398 GHz, 2.415 GHz and 3.491 GHz, respectively. Additionally, it can be seen that from the Figs. 5(b) and (c) the current density of mode I operating at 2.398 GHz reaches the maximum value at the symmetry axis, whereas for the mode II centering

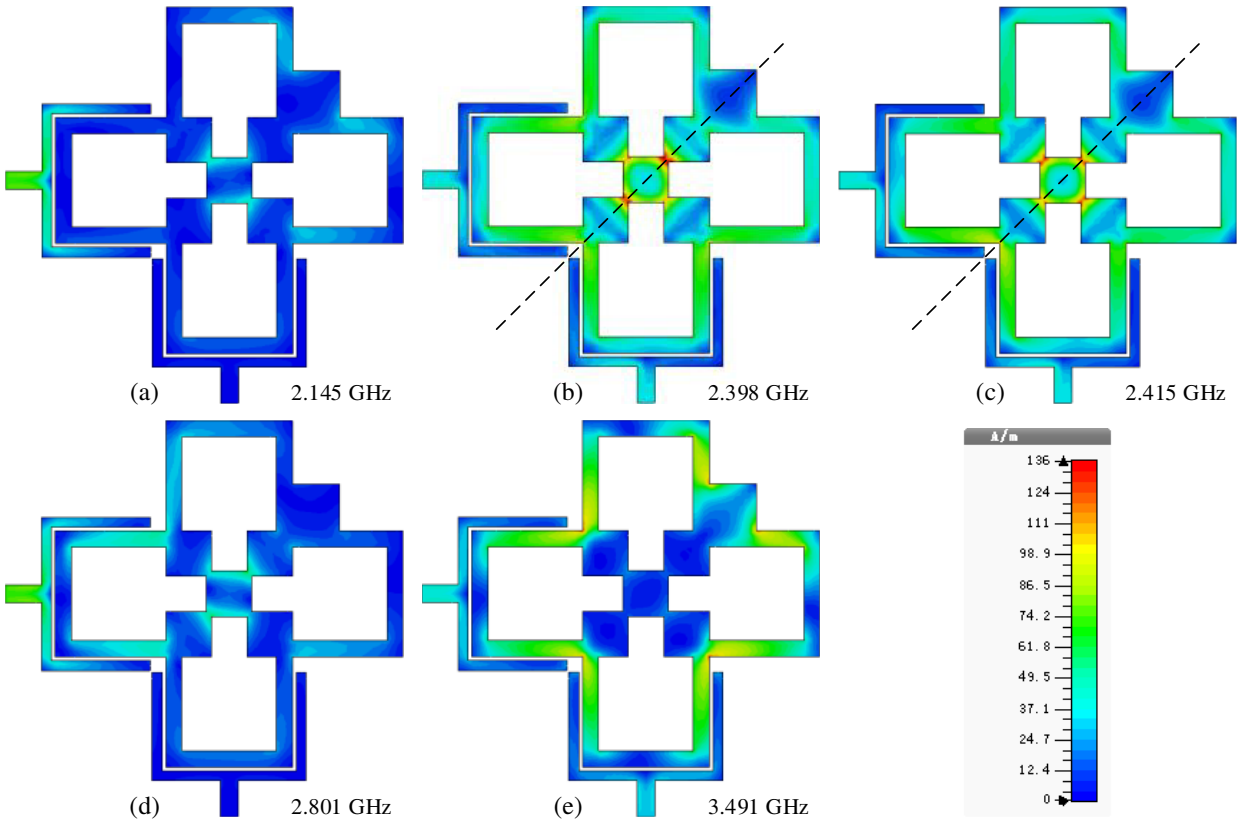

Figure 5: Current density distribution at the surface of the proposed BPF simulated at frequency of (a) 2.145 GHz, (b) 2.398 GHz, (c) 2.415 GHz, (d) 2.801 GHz and (e) 3.491 GHz.

at 2.415 GHz, the current density reaches the maximum value at the position which is orthogonal with the symmetry axis.

5. CONCLUSION

In this paper, a compact dual-mode dual-band microstrip BPF based on typical dual-mode meander loop resonator is designed. The simulated results show that the frequency responses of the proposed BPF have two passbands with center frequency located at 2.407 GHz and 3.491 GHz, respectively. The maximum insertion loss is 0.56 dB, the FBW is 7.3% and the return loss is better than −35 dB from 2.39 GHz to 2.42 GHz in the lower passband, while the maximum insertion loss is 0.62 dB and the FBW is 4.4% in the high passband. What's more, due to the present of two TZs, the proposed BPF has fine frequency selectivity and stopband rejection. Therefore, the proposed BPF can be used for WLAN and WiMAX applications in terms of the performance.

REFERENCES

1. Wolff, I., "Microstrip bandpass filter using degenerate modes of a microstrip ring resonator," *Electronic Letters*, Vol. 8, No. 12, 302–303, 1972.
2. Kim, C. H. and K. Chang, "Ring resonator bandpass filter with switchable bandwidth using stepped-impedance stubs," *IEEE Transactions on Microwave Theory and Techniques*, Vol. 58, No. 12, 3936–3944, 2010.
3. Keshvari, M. and M. Tayarani, "A novel dual-mode dual-band bandpass filter," *Microwave and Optical Technology Letters*, Vol. 53, No. 3, 656–659, 2011.
4. Wang, Y., "Dual-mode dual-passband microstrip bandpass filter with a high selective performance," *Microwave and Optical Technology Letters*, Vol. 53, No. 3, 666–669, 2011.
5. Karpuz, C., A. K. Gorur, and E., Sahin, "Dual-mode dual-band microstrip bandpass filter with controllable center frequency," *IEEE Microwave and Wireless Components Letters*, Vol. 57, No. 3, 639–642, 2015
6. Mandelbrot, B. B., *The Fractal Geometry of Nature*, W. H. Freeman and Company, New York, 1983.

7. Ali, J. K., "A new reduced size multiband patch antenna structure based on Minkowski per-fractal geometry," *Journal of Engineering and Applied Sciences*, Vol. 2, 1120–1124, June 2007.
8. Weng, M.-H., D.-S. Lee, R.-Y. Yang, H.-W. Wu, and C.-L. Liu, "A Sierpinski fractal-based dual-mode bandpass filter," *Microwave and Optical Technology Letters*, Vol. 50, No. 9, 2287–2289, 2008.
9. Li, T.-P., G.-M. Wang, K. Lu H.-X. Xu, Z.-H. Liao, and B.-F. Zong, "Novel bandpass filter based on CSRR using Koch fractal curve," *Progress In Electromagnetics Research Letters*, Vol. 28, 121–128, 2012.
10. Ghatak, R., M. Pal, C. Goswami, and D. R. Poddar, "Moore curve fractal-shaped miniaturized complementary spiral resonator," *Microwave and Optical Technology Letters*, Vol. 55, No. 8, 1950–1954, 2013.
11. Hong, J. S. and M. J. Lancaster, *Microstrip Filters for RF/Microwave Applications*, John Wiley & Sons, Inc., New York, 2001.
12. Ali, J. K., "A new miniaturized fractal bandpass filter based on dual-mode microstrip square ring resonator," *5th International Multi-Conference on Systems, Signals and Devices*, Amman, Jordan, 2008.